Prediction of the Boiling Point, Heat of Vaporization, and Vapor Pressure at Various Temperatures for Polycyclic Aromatic Hydrocarbons

Curt M. White

Division of Coal Science, Pittsburgh Energy Technology Center, Pittsburgh, Pennsylvania 15236

The linear relationship between retention index and normal boiling point is defined for 48 planar polycyclic aromatic hydrocarbons (PAH) and is used to predict (with a standard error of estimate of 6.78 K) the boiling points of 66 other planar PAH. The average percent deviation between the predicted and literature values of the boiling points is 0.68. The heats of vaporization, ΔH_v, of these PAH are predicted by employing Trouton's rule. The average percent deviation between predicted and experimental ΔH_v is 5.1. The quality of these predictions is illustrated by using the boiling point and heat of vaporization information to predict the vapor pressures of naphthalene, 1-methylnaphthalene, phenanthrene, and fluorene using the Clausius-Clapeyron equation. These predicted vapor pressures were compared with experimental values. Lastly, the linear relationships between first-order valence molecular connectivity ($^1\chi_v$, a molecular topological descriptor) and boiling point and ΔH_v of PAH are illustrated. It is shown that $^1\chi_v$ can be used to predict boiling point and ΔH_v of PAH. Reasons for the linear relationship between planar PAH physicochemical properties and $^1\chi_v$ are proposed.

Introduction

Information concerning the fundamental physical, chemical, and thermodynamic properties of coal liquids under a variety of conditions is needed to properly design and operate coal liquefaction plants (*1-4*). The aromatic fraction of coal liquefaction products generally constitutes between 20 and 60 wt % of the whole material (*5*). Distillate cuts of the whole material often contain even larger amounts of the aromatic fraction. The aromatic fraction often consists primarily of polycyclic aromatic hydrocarbons (PAH). Thus, knowledge of the chemical, physical, and thermodynamic properties of individual PAH is important in developing reliable means of estimating the properties of coal liquefaction products. Unfortunately, little information concerning the properties of PAH has been reported, although some data have been tabulated by Herington (*6*). Recently, a large collection of PAH normal boiling points have been compiled by Bjorseth (*7*), Bartle et al. (*8*), and Herington (*6*). Obtaining information on the properties of PAH is particularly valuable because it is thought that coal liquids behave differently from petroleum because of the large mass of aromatics (PAH) present in coal liquids (*1*). The vapor pressure as a function of temperature has been measured for only a few PAH. Almost no vapor pressure data exist for PAH at superatmospheric pressures. Coal liquefaction plants operate at temperatures near 400 °C and at pressures of 200 ktorr and higher. It is at these extreme conditions that vaporization data are ultimately needed. This knowledge is also needed to develop an understanding of the environmental transport and distribution of these organic pollutants. Before accurate models can be developed, reliable information concerning the physical, chemical and thermodynamic properties of PAH is needed.

One purpose of this article is to describe the correlation of PAH boiling points and gas chromatographic retention indices for 48 planar PAH for which boiling points and retention indices are available. This relationship can be used to predict the boiling points of other PAH for which only a retention index is known. Gas chromatographic retention is directly related to vapor pressure and thus to boiling point (*8*). Reid, Prausnitz, and Sherwood correctly note that "methods for estimating boiling points are generally poor" (*9*). Therefore, development of techniques to reliably predict boiling points is needed.

A second purpose of this article is to predict heats of vaporization, ΔH_v, for PAH by using Trouton's rule and the predicted boiling points. The quality of these predictions is illustrated by using them to predict the vapor pressures of PAH at various temperatures and then comparing the predicted vapor pressures with experimental values. Lastly, it will be shown that for individual planar PAH where no experimental information is available, their normal boiling point and heat of vaporization can be predicted by using molecular connectivity calculations (*10*). Development of procedures for the prediction of thermochemical properties of PAH is of considerable recent interest. Stein et al. (*11*) have used group additivity methods for the prediction of standard gas-phase heats of formation, intrinsic entropy, and heat capacity for PAH, whereas Ruzicka has developed a group contribution method for estimation of vapor pressures of aromatic hydrocarbons (*12*).

Results and Discussion

Estimation of PAH Boiling Points from Retention Indices. The linear-temperature-programmed gas chromatographic PAH retention indices for several hundred PAH have been measured at PETC (*5*, *13*, *14*). The relationship between the boiling points of 48 planar PAH and their respective gas chromatographic PAH retention indices is shown in Figure 1. The data used to construct the graph are in Table I. The linear relationship between gas chromatographic retention characteristics and boiling point of PAH is well documented (*8*, *15*). Bartle et al. (*8*) have shown that the slopes of the linear least-squares regression lines describing the relationship between boiling point and PAH retention indices for planar and nonplanar PAH are slightly different. This difference probably results from an entropy effect. The present article considers only planar PAH. Similarly, Borwitzky and Schomburg have shown that the same relationship is slightly different for PAH and for nitrogen-containing PAH (*15*). Even though the relationship between PAH retention index and boiling point is well documented, the compilation of 48 planar PAH boiling points considered here allows this linear relationship to be more clearly defined than previously possible. The boiling points of other planar PAH for which only a PAH retention index is known can be predicted by using the linear least-squares regression line described by eq 1

$$T_b = 1.0672I + 282.82 \quad (1)$$

where T_b is the normal boiling point (K), and I is the PAH retention index in Table I. This regression line (Figure 1), be-

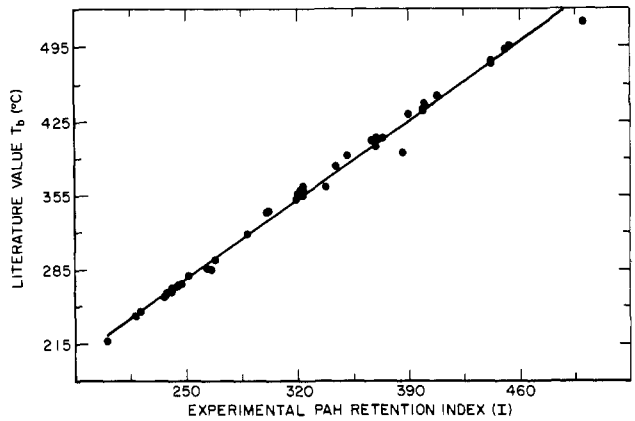

Figure 1. This graph is the linear least-squares regression line describing the relationship between PAH retention index and the literature value of the normal boiling point for 48 planar PAH. The correlation coefficient of the line is 0.997; the standard error of estimate is 6.78 K, and the slope and y intercept are 1.0672 and 282.82 K (9.67 °C), respectively. The data used to construct the graph are in Table I.

tween the literature value of the boiling point and the experimentally determined PAH retention index, has a correlation coefficient of 0.997, and a standard error of estimate of 6.78 K. The average percent deviation is 0.68. The predicted boiling points and those obtained from a literature source (*7*) are presented in Table I, together with the percent deviations. Development of means to predict boiling points is particularly valuable because (a) experimental measurement of the boiling points of PAH is tedious, (b) a large number of these compounds are not commercially available, and (c) they are difficult to synthesize and purify.

Estimation of PAH ΔH_v from Boiling Points and Average Trouton Ratio. The heat of vaporization, ΔH_v, of compounds can be predicted by using Trouton's rule if the respective boiling point and Trouton ratio are known. The heats of vaporization have been measured for 12 PAH (*6*), and these are listed in Table II along with their boiling points. From the experimentally determined values of ΔH_v, and the experimentally determined boiling points, the Trouton ratios for these 12 PAH have been calculated and are listed in Table II. The average Trouton ratio is 22.15 ± 1.34 cal mol^{-1} deg^{-1}. Using this as the Trouton ratio for all planar PAH, and their respective predicted boiling points, it is possible to calculate the ΔH_v. The predicted ΔH_v for planar PAH are in Table I, along with the percent deviation. The average percent deviation is 5.1.

Estimation of PAH Vapor Pressure from the Clausius–Clapeyron Relationship. The present boiling point and ΔH_v information is useful in predicting the vapor pressures of these same PAH at various temperatures. Using the Clausius–Clapeyron relationship (eq 2), the boiling points, and the heats of

$$\log \frac{P_1}{P_2} = \frac{\Delta H_v}{2.303R}\left(\frac{1}{T_2} - \frac{1}{T_1}\right) \qquad (2)$$

vaporization for PAH, it is possible to predict their vapor pressures at various temperatures if the vapor behaves ideally, and if ΔH_v is constant in the temperature range of the predictions. In eq 2, P_1 is the vapor pressure at T_1, P_2 is the vapor pressure at T_2, and ΔH_v is the heat of vaporization. To obtain a measure of the reliability of such an approach, the predicted vapor pressures at various temperatures and those determined experimentally by Wilson et al. (*1*) for naphthalene are in Table III, along with their average percent deviation. The experimental and predicted relationships are graphically illustrated in Figure 2. The average percent deviation between the experimental values and those predicted by Clausius–Clapeyron using the predicted ΔH_v and experimental normal boiling points is 8.18; the average percent deviation obtained by using the

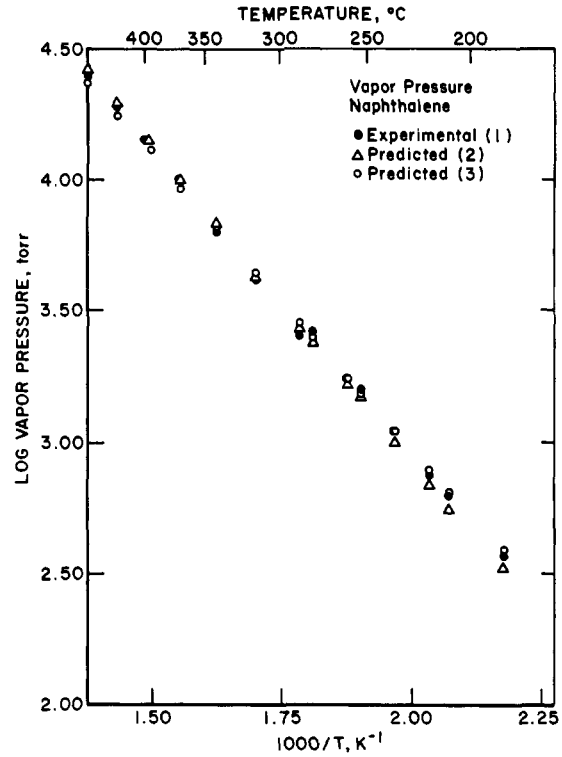

Figure 2. Description of the relationship between the log of the vapor pressure (torr) and $1/T$ (K) for naphthalene. Line 1 is the experimentally determined relationship, while line 2 is the relationship predicted by employing the Clausius–Clapeyron equation and using the predicted ΔH_v and the predicted boiling point. Line 3 is the relationship predicted by employing the Clausius–Clapeyron equation using the experimental ΔH_v and the experimental boiling point. The values between the points were interpolated. The data used to construct the graph are in Table III. The experimental data were obtained by Wilson et al. (*1*).

experimentally determined ΔH_v and experimentally determined normal boiling points is 3.94; and the average percent deviation obtained by using the predicted ΔH_v and predicted normal boiling point is 5.51. The predicted vapor pressures at various temperatures and those determined experimentally by Sivaraman and Kobayashi (*16*) and by Wilson et al. (*1*) are given in Figures 5, 6, and 7 and in Tables V, VI, and VII available as supplementary material for fluorene, 1-methylnaphthalene and phenanthrene, respectively. (See Supplementary Material Available paragraph at the end of this article.)

Estimation of PAH Boiling Points and ΔH_v Using Molecular Connectivity. Coal liquefaction products contain hundreds of PAH that have not yet been identified. Additionally, coal liquids contain PAH for which no PAH retention index has been measured. The ability to predict the physical, chemical, and thermodynamic properties of these compounds is needed. First-order valence molecular connectivity is an easily calculated topological parameter extensively developed by Kier and Hall (*10*). Molecular connectivity is a description of molecular structure based on a count of groupings of skeletal atoms, weighted by degree of skeletal branching. The first-order valence molecular connectivity, $^1\chi_v$, is calculated according to eq 3. Each vertex (atom) of the molecular graph of a compound

$$^1\chi_v = \sum(\delta_i\delta_j)^{-1/2} \qquad (3)$$

is assigned a value (δ), which is the number of bonds to that atom, ignoring bonds attached to hydrogen. The summation includes all bonds in the molecular graph except those to hydrogen. Atoms i and j are bonded. An example calculation of $^1\chi_v$ for phenanthrene is shown in Figure 3. The calculated first-order valence molecular connectivities, $^1\chi_v$, of 47 planar PAH are in Table I (*17*, *18*). The linear least-squares re-

Table I. Retention Indices, Boiling Points, Heats of Vaporization, and First-Order Valence Molecular Connectivities of Planar PAH

	planar PAH[a]	expt I	stand. dev	T_b, K lit.[b]	T_b, K pred.[f]	% dev[e,f]	ΔH_v, kJ mol^{-1} exptl	ΔH_v, kJ mol^{-1} pred[f,g]	% dev[e,f]	$^1\chi_v$[d]
1.	naphthalene	200.00		491	496	1.0	43.18	45.99	6.5	3.405
2.	2-methylnaphthalene	218.14	0.28	514	516	0.3		47.78		3.815
3.	azulene	219.95	0.24		518			47.96		3.405
4.	1-methylnaphthalene	221.04	0.25	518	519	0.1		48.07		3.822
5.	2-ethylnaphthalene	236.08	0.16	531	535	0.7		49.56		
6.	1-ethylnaphthalene	236.56	0.14	532	535	0.6		49.61		
7.	2,6-dimethylnaphthalene	237.58	0.17	535	536	0.2	48.71	49.71	2.1	
8.	2,7-dimethylnaphthalene	237.71	0.07	535	536	0.3	48.77	49.72	1.9	
9.	1,3-dimethylnaphthalene	240.25	0.16	538	539	0.2		49.97		
10.	1,7-dimethylnaphthalene	240.66	0.25	536	540	0.7	48.77	50.01	2.5	
11.	1,6-dimethylnaphthalene	240.72	0.09	539	540	0.1	48.77	50.02	2.6	
12.	2,3-dimethylnaphthalene	243.55	0.19	541	543	0.3	48.98	50.30	2.7	
13.	1,4-dimethylnaphthalene	243.57	0.16	541	543	0.3		50.30		
14.	1,5-dimethylnaphthalene	244.98	0.16	542	544	0.4		50.44		
15.	acenaphthylene	244.63	0.19	543	544	0.1		50.40		4.149
16.	1,2-dimethylnaphthalene	246.49	0.30	544	546	0.3		50.59		
17.	1,8-dimethylnaphthalene	249.52			549			50.89		
18.	acenaphthene	251.29	0.14	552	551	0.2		51.06		4.445
19.	2,3,6-trimethylnaphthalene	263.31	0.12	559	564	0.8		52.25		
20.	1-methylacenaphthylene	265.24	0.02		566			52.44		
21.	2,3,5-trimethylnaphthalene	265.90	0.14	558	567	1.5		52.51		
22.	fluorene	268.17	0.15	567	569	0.3	58.15	52.73	9.3	4.611
23.	9-methylfluorene	272.38	0.17		573			53.15		
24.	9-ethylfluorene	284.99	0.20		587			54.40		
25.	2-methylfluorene	288.21	0.15	591	590	0.1		54.71		
26.	1-methylfluorene	289.03	0.04		591			54.80		
27.	1,2,3,4-tetrahydrophenanthrene	297.21			600			55.60		
28.	phenanthrene	300.00		611	603	1.3	52.72	55.88	6.0	4.815
29.	anthracene	301.69	0.08	613	605	1.4	52.35	56.05	7.1	4.809
30.	1,2,3,10b-tetrahydrofluoranthene	316.37	0.14		620			57.50		
31.	9-*n*-propylfluorene	318.01	0.20		622			57.66		
32.	3-methylphenanthrene	319.46	0.12	625	624	0.2		57.81		5.226
33.	2-methylphenanthrene	320.17	0.12	628	624	0.6		57.88		5.226
34.	2-methylanthracene	321.57	0.12	632	626	1.0		58.01		5.220
35.	4*H*-cyclopenta[*def*]phenanthrene	322.08	0.15	632	627	0.9		58.06		5.356
36.	9-methylphenanthrene	323.06	0.24	628	628	0.1		58.16		5.232
37.	4-methylphenanthrene	323.17			628			58.17		5.232
38.	1-methylanthracene	323.33		636	628	1.3		58.19		
39.	1-methylphenanthrene	323.90	0.08	632	628	0.6		58.24		5.226
40.	9-*n*-butylfluorene	328.99	0.37		634			58.75		
41.	9-methylanthracene	329.13	0.19		634			58.76		5.232
42.	4,5-dihydropyrene	330.01	0.02		635			58.85		
43.	9-ethylphenanthrene	337.05	0.08		643			59.54		
44.	2-ethylphenanthrene	337.50			643			59.59		
45.	3,6-dimethylphenanthrene	337.83	0.14	636	643	1.1		59.62		5.649
46.	2,7-dimethylphenanthrene	339.23	0.16		645			59.76		
47.	1,2,3,6,7,8-hexahydropyrene	339.38	0.17		645			59.78		
48.	fluoranthene	344.01	0.16	656	650	1.0	66.52	60.23	9.5	5.565
49.	9-isopropylphenanthrene	345.78	0.28		652			60.41		
50.	1,8-dimethylphenanthrene	346.26	0.27		652			60.46		
51.	9-*n*-hexylfluorene	348.54	0.10		655			60.68		
52.	9-*n*-propylphenanthrene	350.30	0.17		657			60.86		
53.	pyrene	351.22	0.08	666	658	1.3	65.81	60.95	6.0	5.559
54.	9,10-dimethylanthracene	355.49	0.03		662			61.37		
55.	9-methyl-10-ethylphenanthrene	359.91	0.19		667			61.81		
56.	benzo[*a*]fluorene	366.74	0.13	680	674	0.9		62.48		6.022
57.	11-methylbenzo[*a*]fluorene	367.04	0.14		675			62.51		
58.	9,10-diethylphenanthrene	367.97	0.15		676			62.60		
59.	1-methyl-7-isopropylphenanthrene	368.67	0.19		676			62.67		
60.	benzo[*b*]fluorene	369.39	0.15	675	677	0.3		62.74		6.016
61.	4-methylpyrene	369.54	0.13	683	677	0.9		62.76		5.970
62.	2-methylpyrene	370.15	0.44	683	678	0.8		62.82		
63.	4,5,6-trihydrobenz[*de*]anthracene	370.86			679			62.89		
64.	1-methylpyrene	373.55	0.11	683	681	0.3		63.15		5.976
65.	9,10-dimethyl-3-ethylphenanthrene	381.85	0.18		690			63.98		
66.	1-ethylpyrene	385.35			694			64.32		
67.	2,7-dimethylpyrene	386.34	0.06	669	695	3.9		64.42		
68.	benzo[*ghi*]fluoranthene	389.60	0.06	705	699	0.9		64.74		6.309
69.	benzo[*c*]phenanthrene	391.39	0.40		700			64.92		6.226
70.	cyclopenta[*cd*]pyrene	396.54	0.08		706			65.43		6.303
71.	benz[*a*]anthracene	398.50	0.08	708	708	0.0		65.62		6.220
72.	chrysene	400.00		714	710	0.6	69.54	65.77	5.4	6.226
73.	triphenylene	400.00	0.01	712	710	0.4		65.77		6.232
74.	naphthacene	408.30	0.22	723	719	0.6		66.59		

Table I (Continued)

	planar PAH[a]	expt I	stand. dev	T_b, K lit.[b]	T_b, K pred.[f]	% dev[e,f]	ΔH_v, kJ mol^{-1} exptl	ΔH_v, kJ mol^{-1} pred[f,g]	% dev[e,f]	$^1\chi_v$[d]
75.	11-methylbenz[a]anthracene	412.72			723			67.03		
76.	2-methylbenz[a]anthracene	413.78	0.44		724			67.13		
77.	1-methylbenz[a]anthracene	414.37	0.17		725			67.19		
78.	1-*n*-butylpyrene	414.87	0.12		726			67.24		
79.	1-methyltriphenylene	416.32			727			67.38		
80.	9-methylbenz[a]anthracene	416.50	0.20		727			67.40		
81.	3-methylbenz[a]anthracene	416.63			727			67.42		
82.	8-methylbenz[a]anthracene	417.56	0.04		728			67.51		
83.	6-methylbenz[a]anthracene	417.57	0.30		728			67.51		
84.	3-methylchrysene	418.10	0.17		729			67.56		
85.	5-methylbenz[a]anthracene	418.72			730			67.62		
86.	2-methylchrysene	418.80			730			67.63		
87.	12-methylbenz[a]anthracene	419.39	0.45		730			67.69		6.642
88.	4-methylbenz[a]anthracene	419.67			731			67.72		
89.	5-methylchrysene	419.68			731			67.72		
90.	6-methylchrysene	420.61	0.04		732			67.81		
91.	4-methylchrysene	420.83	0.16		732			67.83		
92.	1-methylchrysene	422.87	0.06		734			68.03		
93.	7-methylbenz[a]anthracene	423.14			734			68.06		6.642
94.	1,3-dimethyltriphenylene	432.32			744			68.97		
95.	1,12-dimethylbenz[a]anthracene	436.82			749			69.41		
96.	benzo[j]fluoranthene	440.92			753			69.82		6.976
97.	benzo[b]fluoranthene	441.74	0.48	754	754	0.0		69.90		6.976
98.	benzo[k]fluoranthene	442.56		754	755	0.1		69.98		6.970
99.	7,12-dimethylbenz[a]anthracene	443.38	0.12		756			70.06		
100.	1,6,11-trimethyltriphenylene	446.24			759			70.34		
101.	benzo[e]pyrene	450.73	0.17	766	764	0.3		70.79		6.975
102.	benzo[a]pyrene	453.44		769	767	0.3		71.06		6.976
103.	perylene	456.22	0.29		770			71.33		6.976
104.	1,3,7,11-tetramethyltriphenylene	461.72			776			71.87		
105.	3-methylcholanthrene	468.44			783			72.54		7.685
106.	indeno[1,2,3-cd]pyrene	481.87	0.09		797			73.87		7.720
107.	pentacene	486.81			802			74.36		7.619
108.	dibenz[a,c]anthracene	495.01	0.08		811			75.17		7.637
109.	dibenz[a,h]anthracene	495.45			812			75.21		7.631
110.	benzo[b]chrysene	497.66			814			75.43		7.631
111.	picene	500.00		792	816	3.1		75.66		7.637
112.	benzo[ghi]perylene	501.32	0.18		818			75.79		7.720
113.	dibenzo[def,mno]chrysene	503.89			821			76.05		7.714
114.	2,3-dihydrodibenzo[def,mno]chrysene	503.91			821			76.05		

[a] Planar PAH are those compounds having more than one aromatic ring where all aromatic rings are coplanar. [b] All normal boiling points were taken from ref 7 unless otherwise noted. The normal boiling points in ref 7 are valid at 1 atm (unless otherwise indicated) and thus did not have to be corrected. The boiling point information compiled in ref 7 and used here was taken from ref 21–24. (Personal communication, Alf Bjorseth, 84/08/14.) [d] Taken from ref 17 and 18. [e] |exptl − pred|/exptl × 100 = percent deviation. [f] The predicted values and percent deviations were calculated by carrying all digits (significant and otherwise) through the entire calculation and rounding the final answer. [g] Calculated by using Trouton's rule with the average Trouton constant and the predicted boiling points. These values should be rounded to three significant figures before use.

Table II. Experimental Heats of Vaporization, Boiling Points, and Calculated Trouton Ratios for 12 PAH[a]

	compd	exptl[b] ΔH_v, kJ mol^{-1}	T_b, K	Trouton ratio,[c] cal mol^{-1} deg^{-1}
1.	anthracene	52.35	614.5	20.4
2.	chrysene	69.54	721	23.1
3.	1,6-dimethylnaphthalene	48.77	538	21.7
4.	1,7-dimethylnaphthalene	48.77	535	21.8
5.	2,3-dimethylnaphthalene	48.98	542	21.6
6.	2,6-dimethylnaphthalene	48.71	535	21.8
7.	2,7-dimethylnaphthalene	48.77	535	21.8
8.	fluoranthene	66.52	656[d]	24.2
9.	fluorene	58.15	567	24.5
10.	naphthalene	43.18	491	21.0
11.	phenanthrene	52.72	611	20.6
12.	pyrene	65.81	666	23.3

[a] Data taken from ref 6 unless otherwise noted. [b] These values have been rounded to the appropriate number of significant figures. [c] The ΔH_v values before rounding were used to calculate these Trouton ratios. [d] Taken from ref 7.

gression line describing the relationship between the literature value of the normal boiling points, in kelvin, and $^1\chi_v$ for the 30 planar PAH for which both values are available has a correlation coefficient of 0.994 and a standard error of estimate of 8.59 K. The relation is described in eq 4. The normal boiling point,

$$T_b = 76.21\,^1\chi_v + 225.71 \quad (4)$$

in kelvin, of a planar PAH can be estimated by calculating its first-order valence molecular connectivity according to eq 3 and Figure 3, and substituting this value into eq 4. When the normal boiling points are expressed in kelvin, the average percent deviation between the literature and predicted values is 1.22. A graph of $^1\chi_v$ as a function of the literature value of the normal boiling point is shown in Figure 8 of the supplementary material. Thus, it is possible to estimate a normal boiling point of a planar PAH for which no experimental information is available. Similarly, $^1\chi_v$ and ΔH_v are linearly related. The linear least-squares regression line between the predicted ΔH_v and calculated $^1\chi_v$ for 47 planar PAH in Table I for which both values are available is shown in Figure 9 of the supplementary material. This line has a correlation coefficient of 0.993 and standard error of estimate of 9.39 kJ mol^{-1}, and is described by eq 5. The ΔH_v

$$\Delta H_v = 6.464\,^1\chi_v + 25.147 \quad (5)$$

of a planar PAH can be estimated by calculating its first-order

Table III. Predicted and Experimental Vapor Pressures of Naphthalene at Various Temperatures[a]

temp		vapor pressure, torr		
°F	°C	exptl	pred[f,g]	% dev[d,e,f]
334.7	168.2	216	191	11.72
372.3	189.1	372	336	9.72
410.7	210.4	626	569	9.18
426.6	219.2	765	697	8.84
455.6	235.3	1090	995	8.72
488.9	253.8	1590	1460	8.36
537.9	281.1	2620	2442	6.79
500[b]	260[b]	1720[c]	1650	4.03
550	288	2660[c]	2760	3.78
600	316	4300[c]	4410	2.51
650	343	6460[b,c]	6650	2.91
700	371	9870	9820	0.54
750	399	14000	14000	0.23
800	427	19100	19500	2.06
850	454	25300	26100	3.28

[a] Experimental values were taken from supplementary material of Wilson et al. (*1*). [b] This point and subsequent points measured in flow cell without hydrogen (*1*). [c] These points are suspected to be too low. [d] |exptl − pred|/exptl × 100 = percent deviation. [e] The average percent deviation between the experimental vapor pressures and those predicted in this column is 5.51. [f] The calculated values and percent deviations were calculated carrying all digits (significant and otherwise) through the entire calculation and rounding the final answer. [g] Predicted from predicted ΔH_v and predicted T_b.

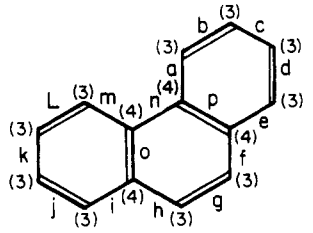

$$^1\chi_V = \underset{a}{\sqrt{\frac{1}{4\cdot3}}} + \underset{b}{\sqrt{\frac{1}{3\cdot3}}} + \underset{c}{\sqrt{\frac{1}{3\cdot3}}} + \underset{d}{\sqrt{\frac{1}{3\cdot3}}} + \underset{e}{\sqrt{\frac{1}{3\cdot4}}}$$

$$+ \underset{f}{\sqrt{\frac{1}{4\cdot3}}} + \underset{g}{\sqrt{\frac{1}{3\cdot3}}} + \underset{h}{\sqrt{\frac{1}{3\cdot4}}} + \underset{i}{\sqrt{\frac{1}{4\cdot3}}} + \underset{j}{\sqrt{\frac{1}{3\cdot3}}}$$

$$+ \underset{k}{\sqrt{\frac{1}{3\cdot3}}} + \underset{L}{\sqrt{\frac{1}{3\cdot3}}} + \underset{m}{\sqrt{\frac{1}{3\cdot4}}} + \underset{n}{\sqrt{\frac{1}{4\cdot4}}} + \underset{o}{\sqrt{\frac{1}{4\cdot4}}}$$

$$+ \underset{p}{\sqrt{\frac{1}{4\cdot4}}} = 4.815$$

Figure 3. An example calculation of the first-order valence molecular connectivity of phenanthrene. Numbers in parentheses are the assigned δ values of the individual atoms. Bonds around the molecule are lettered to facilitate the calculations.

valence molecular connectivity according to eq 3 and Figure 3, and substituting this value into eq 5. The average percent deviation between predicted ΔH_v using eq 5 and the predicted ΔH_v in Table I is 1.54.

The correlation between the first-order valence molecular connectivity of PAH with their physical, chemical, and thermodynamic properties is not surprising. The properties of PAH are a direct function of their size and topology. These relationships have been discussed recently by Zander (*19*). Size is a function of the number of π-electrons, while topology is related to whether the ring systems are kata-annellated or peri-condensed. Topology is also a function of linear and angular ring annelation (*20*). The PAH size and topology affect the energy of the highest occupied molecular orbital (HOMO), which in turn

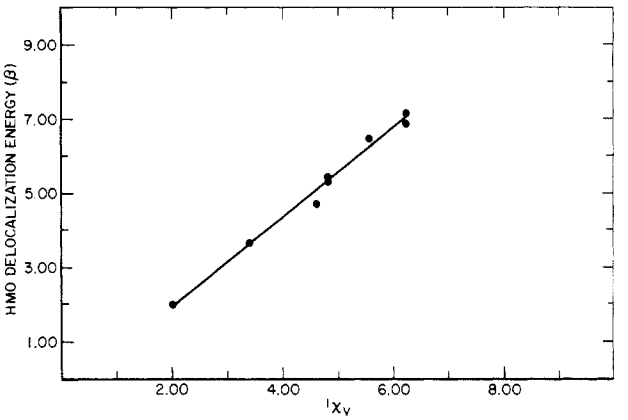

Figure 4. Linear least-squares regression line illustrating the relationship between $^1\chi_v$ and delocalization energy of benzene and seven planar PAH. The correlation coefficient is 0.995, and the standard error of estimate is 0.20β, while the slope and y intercept are 1.22 and −0.49 β. Data used to construct the graph are in Table IV.

Table IV. First-Order Valence Molecular Connectivity, Delocalization Energy, and Calculated van der Waals Volumes of Benzene and Some Planar PAH[a]

	compd	calcd van der Waals vol, cm^3 mol^{-1}	$^1\chi_v$	delocaln energy β
1.	benzene	48.36	2.000	2.000
2.	naphthalene	73.96	3.405	3.683
3.	fluorene	93.22	4.611	4.75
4.	phenanthrene	99.56	4.815	5.448
5.	anthracene	99.56	4.809	5.314
6.	pyrene	109.04	5.559	6.506
7.	chrysene	125.16	6.226	7.190
8.	tetracene	125.16	6.214	6.932
9.	benzo[*a*]pyrene	134.64	6.970	
10.	pentacene	150.76	7.619	

[a] Delocalization energies were taken from the literature (*25–27*), while the van der Waals volumes were calculated by Hanai and Hubert (*28*).

is a reasonable predictor of their properties. In fact, there is a linear relationship between $^1\chi_v$ and both the Hückel molecular orbital (HMO) delocalization energy as shown in Figure 4 and calculated van der Waals volume of benzene and planar PAH as shown in Figure 10 of the supplementary material (see Table IV). Consequently, T_b, ΔH_v, $^1\chi_v$, I, the energy of the HOMO, the HMO delocalization energy, and van der Waals volume of planar PAH are all linearly related. Discovery of these relationships greatly facilitates the prediction of the physical, chemical, and thermodynamic properties of PAH, and thus facilitates prediction of these properties for coal-derived liquids.

Glossary

ΔH_v	heat of vaporization, cal mol^{-1}, kJ mol^{-1}
T_b	normal boiling point, K
I	PAH retention index
$^1\chi_v$	first-order valence molecular connectivity
β	π-electron energy
P_1	vapor pressure at temperature 1 (760 torr at the T_b), torr
P_2	vapor pressure at temperature 2, torr
T_1	temperature 1 (T_b), K
T_2	temperature 2, K

Acknowledgment

I thank Margie Farabaugh for performing the calculations used in this article. I thank M. B. Perry, M. Edmunds, R. F. Sprecher, D. Finseth, M. L. Lee, K. D. Bartle, G. M. Wilson, B.

Gammon, J. Winnick, and D. Eatough for many helpful discussions.

Registry No. 2-Methylnaphthalene, 91-57-6; azulene, 275-51-4; 1-methylnaphthalene, 90-12-0; 2-ethylnaphthalene, 939-27-5; 1-ethylnaphthalene, 1127-76-0; 1,3-dimethylnaphthalene, 575-41-7; 1,4-dimethylnaphthalene, 571-58-4; 1,5-dimethylnaphthalene, 571-61-9; acenaphthylene, 208-96-8; 1,2-dimethylnaphthalene, 573-98-8; 1,8-dimethylnaphthalene, 569-41-5; acenaphthene, 83-32-9; 2,3,6-trimethylnaphthalene, 829-26-5; 1-methylacenaphthylene, 19345-99-4; 2,3,5-trimethylnaphthalene, 2245-38-7; 9-methylfluorene, 2523-37-7; 9-ethylfluorene, 2294-82-8; 2-methylfluorene, 1430-97-3; 1-methylfluorene, 1730-37-6; 1,2,3,4-tetrahydrophenanthrene, 1013-08-7; 1,2,3,10-tetrahydrofluoranthene, 100701-62-0; 9-propylfluorene, 4037-45-0; 3-methylphenanthrene, 832-71-3; 2-methylphenanthrene, 2531-84-2; 2-methylanthracene, 613-12-7; 4*H*-cyclopenta[*def*]phenanthrene, 203-64-5; 9-methylphenanthrene, 883-20-5; 4-methylphenanthrene, 832-64-4; 1-methylanthracene, 610-48-0; 1-methylphenanthrene, 832-69-9; 9-butylfluorene, 3952-42-9; 9-methylanthracene, 779-02-2; 4,5-dihydropyrene, 6628-98-4; 9-ethylphenanthrene, 3674-75-7; 2-ethylphenanthrene, 3674-74-6; 3,6-dimethylphenanthrene, 1576-67-6; 2,7-dimethylphenanthrene, 1576-69-8; 1,2,3,6,7,8-hexahydropyrene, 1732-13-4; 9-isopropylphenanthrene, 17024-04-3; 1,8-dimethylphenanthrene, 7372-87-4; 9-hexylfluorene, 2470-83-9; 9-propylphenanthrene, 17024-03-2; 9,10-dimethylanthracene, 781-43-1; 9-methyl-10-ethylphenanthrene, 17024-02-1; benzo[*a*]fluorene, 30777-18-5; 11-methylbenzo[*a*]fluorene, 100683-77-0; 9,10-diethylphenanthrene, 15810-14-7; 1-methyl-7-isopropylphenanthrene, 483-65-8; benzo[*b*]fluorene, 30777-19-6; 4-methylpyrene, 3353-12-6; 2-methylpyrene, 3442-78-2; 4,5,6-trihydrobenz[*de*]anthracene, 4389-09-7; 1-methylpyrene, 2381-21-7; 9,10-dimethyl-3-ethylphenanthrene, 1576-64-3; 1-ethylpyrene, 17088-22-1; 2,7-dimethylpyrene, 15679-24-0; benzo[*ghi*]fluoranthene, 203-12-3; benzo[*c*]phenanthrene, 195-19-7; cyclopenta[*cd*]pyrene, 27208-37-3; benz[*a*]anthracene, 56-55-3; triphenylene, 217-59-4; naphthacene, 92-24-0; 11-methylbenz[*a*]anthracene, 6111-78-0; 2-methylbenz[*a*]anthracene, 2498-76-2; 1-methylbenz[*a*]anthracene, 2498-77-3; 1-butylpyrene, 35980-18-8; 1-methyltriphenylene, 2871-91-2; 9-methylbenz[*a*]anthracene, 2381-16-0; 3-methylbenz[*a*]anthracene, 2498-75-1; 8-methylbenz[*a*]anthracene, 2381-31-9; 6-methylbenz[*a*]anthracene, 316-14-3; 3-methylchrysene, 3351-31-3; 5-methylbenz[*a*]anthracene, 2319-96-2; 2-methylchrysene, 3351-32-4; 12-methylbenz[*a*]anthracene, 2422-79-9; 4-methylbenz[*a*]anthracene, 316-49-4; 5-methylchrysene, 3697-24-3; 6-methylchrysene, 1705-85-7; 4-methylchrysene, 3351-30-2; 1-methylchrysene, 3351-28-8; 7-methylbenz[*a*]anthracene, 2541-69-7; 1,3-dimethyltriphenylene, 17157-14-1; 1,12-dimethylbenz[*a*]anthracene, 313-74-6; benzo[*j*]fluoranthene, 205-82-3; benzo[*b*]fluoranthene, 205-99-2; benzo[*k*]fluoranthene, 207-08-9; 7,12-dimethylbenz[*a*]anthracene, 57-97-6; 1,6,11-trimethyltriphenylene, 1156-61-2; benzo[*e*]pyrene, 192-97-2; benzo[*a*]pyrene, 50-32-8; perylene, 198-55-0; 1,3,7,11-tetramethyltriphenylene, 100701-63-1; 3-methylcholanthrene, 56-49-5; indeno[1,2,3-*cd*]pyrene, 193-39-5; pentacene, 135-48-8; dibenz[*a*,*c*]anthracene, 215-58-7; dibenz[*a*,*b*]anthracene, 53-70-3; benzo[*b*]chrysene, 214-17-5; picene, 213-46-7; benzo[*ghi*]perylene, 191-24-2; dibenzo[*def*,*mno*]chrysene, 191-26-4; 2,3-dihydrodibenzo[*def*,*mno*]chrysene, 100701-64-2.

Literature Cited

(1) Wilson, G. M.; Johnston, R. H.; Hwang, S. C.; Tsonopoulos, C. *Ind. Eng. Chem., Process Des. Dev.* **1981**, *20*, 94.
(2) Gray, J. A.; Brady, C. J.; Cunningham, J. R.; Freeman, J. R.; Wilson, G. M. *Ind. Eng. Chem., Process Des. Dev.* **1983**, *22*, 410.
(3) Mraw, S. C.; Heldman, J. L.; Hwang, S. C.; Tsonopoulos, C. *Ind. Eng. Chem., Process Des. Dev.* **1984**, *23*, 577.
(4) Holder, G. D.; Gray, J. A. *Ind. Eng. Chem., Process Des. Dev.* **1983**, *22*, 424.
(5) White, C. M. In "Handbook of Polycyclic Aromatic Hydrocarbons"; Bjorseth, A., Ed.; Marcel Dekker: New York, 1983.
(6) Herington, E. F. G. "Physical Properties of Some Constituents of Coal Tar"; National Physical Laboratory Report Chem. 102, June 1979.
(7) Bjorseth, A., Ed. "Handbook of Polycyclic Aromatic Hydrocarbons"; Marcel Dekker: New York, 1983; Appendix.
(8) Bartle, K. D.; Lee, M. L.; Wise, S. A. *Chromatographia* **1981**, *14*, 69.
(9) Reid, R. C.; Prausnitz, J. M.; Sherwood, T. K. "The Properties of Gases and Liquids"; McGraw-Hill: New York, 1977.
(10) Kier, L. B.; Hall, L. H. "Molecular Connectivity in Chemistry and Drug Research"; Academic Press: New York, 1976.
(11) Stein, S. E.; Golden, D. M.; Benson, S. W. *J. Phys. Chem.* **1977**, *81*, 314.
(12) Ruzicka, V., Jr. *Ind. Eng. Chem. Fundam.* **1983**, *22*, 267.
(13) White, C. M.; Sharkey, A. G.; Lee, M. L.; Vassilaros, D. L. "Polynuclear Aromatic Hydrocarbons", 2nd ed.; Jones, P. W., Leber, P. Eds.; Ann Arbor Science: Ann Arbor, MI, 1979.
(14) Lee, M. L.; Vassilaros, D. L.; White, C. M.; Novotny, M. *Anal. Chem.* **1979**, *51*, 768.
(15) Borwitzky, H.; Schomburg, G. *J. Chromatogr.* **1979**, *170*, 99.
(16) Sivaraman, A.; Kobayashi, R. *J. Chem. Eng. Data* **1982**, *27*, 264.
(17) Doherty, P. J.; Hoes, R. M.; Robbat, A., Jr.; White, C. M. *Anal. Chem.* **1984**, *56*, 2697.
(18) Kaliszan, R.; Lamparczyk, H. *J. Chromatogr. Sci.* **1978**, *20*, 246.
(19) Zander, M. In "Handbook of Polycyclic Aromatic Hydrocarbons"; Bjorseth, A., Ed.; Marcel Dekker: New York, 1983.
(20) Zander, M. "Polycyclische Aromatische Kohlenwasserstoffe"; VDI-Verlag: Dusseldorf, West Germany; VDI-Bericht No. 358.
(21) Lang, K. F.; Eigen, I. *Fort Schritte der Chemischen Forschung* **1987**, *8*, 91–170.
(22) Blokzijl, P. J.; Guicherit, R. TNO-nieuws, 653-660 November 1972. (Research Institute for Public Health Engineering TNO, Schoemakerstraat 97, Delft, The Netherlands.)
(23) Committee on Biologic Effects of Atmospheric Pollutants. "Particulate Polycyclic Organic Matter"; National Academy of Sciences: Washington, DC, 1972.
(24) Grimmer, G. In "Luftqaalitäts-Kriterien für Ausgewählte Polyzylklische Aromatische Kohlenwasserstoffe, Berichte"; Erich Schmidt Verlag: West Berlin, 1979.
(25) Streuli, C. A.; Orloff, M. *J. Chromatogr.* **1971**, *62*, 73.
(26) Ecknig, W.; Trung, B.; Radeglia, R.; Gross, U. *Chromatographia* **1982**, *16*, 1978.
(27) Streitweiser, A., Jr. "Molecular Orbital Theory for Organic Chemists"; Wiley: New York, 1961; p 241.
(28) Hanai, T.; Hubert, J. *J. Chromatogr.* **1984**, *290*, 197.

Received for review February 25, 1985. Revised manuscript received August 28, 1985. Accepted October 28, 1985.

Supplementary Material Available: Tables V–VII and Figures 5–10 (9 pages). The tables consist of the predicted and experimental vapor pressures of fluorene, 1-methylnaphthalene, and phenanthrene, respectively, at various temperatures. These same relationships are depicted graphically in Figures 5–7. A graph of the linear least-squares regression line describing the relationship between first-order valence molecular connectivity ($^1\chi_v$) and the literature value of the normal boiling point for 30 planar PAH for which both values are available is presented in Figure 8. A graph of the linear least-squares regression line describing the relationship between the predicted ΔH_v values and the first-order valence molecular connectivity ($^1\chi_v$) of 47 planar PAH for which both values are available is presented in Figure 9. Lastly, a graph of the linear least-squares regression line illustrating the relationship between first-order valence molecular connectivity ($^1\chi_v$) and calculated van der Waals volume of benzene and nine planar PAH is illustrated in Figure 10. Ordering information is given on any current masthead page.